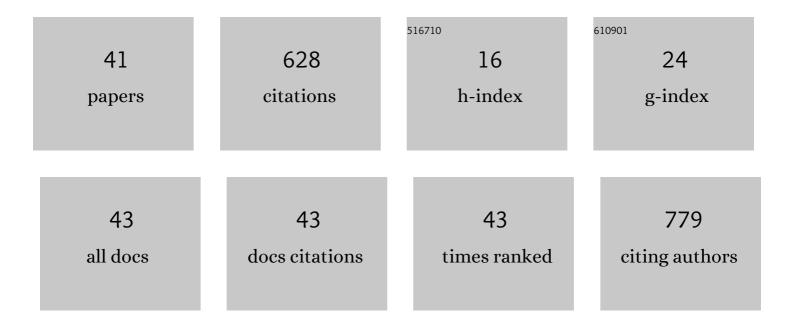
Andrzej Ostrowski

List of Publications by Year in descending order

Source: https://exaly.com/author-pdf/2895383/publications.pdf Version: 2024-02-01



#	Article	IF	CITATIONS
1	Systematic Studies on Liquid Sodium 4,5â€dicyanoâ€2â€(trifluoromethyl)imidazolate (NaTDI)â€Based Electrolytes and Its Impact on the Cycling Behaviour Against Wet Impregnated WIâ€NaNMC and Prussian White Cathodes. Advanced Materials Interfaces, 2022, 9, .	3.7	4
2	Indium(II) Chloride as a Precursor in the Synthesis of Ternary (Ag–In–S) and Quaternary (Ag–In–Zn–S) Nanocrystals. Chemistry of Materials, 2022, 34, 809-825.	6.7	7
3	Development of cobalt catalyst supported on MgO–Ln2O3 (Ln = La, Nd, Eu) mixed oxide systems for ammonia synthesis. International Journal of Hydrogen Energy, 2022, 47, 6666-6678.	7.1	16
4	Influence of substituents in aryl groups on the structure, thermal transitions and electrorheological properties of zinc bis(diarylphosphate) hybrid polymers. Dalton Transactions, 2022, , .	3.3	1
5	Suppressing Ni/Li disordering in LiNi0.6Mn0.2Co0.2O2 cathode material for Li-ion batteries by rare earth element doping. Energy Reports, 2022, 8, 3995-4005.	5.1	22
6	Influence of the Support Composition on the Activity of Cobalt Catalysts Supported on Hydrotalcite-Derived Mg-Al Mixed Oxides in Ammonia Synthesis. Chemistry, 2022, 4, 480-493.	2.2	0
7	A high performance barium-promoted cobalt catalyst supported on magnesium–lanthanum mixed oxide for ammonia synthesis. RSC Advances, 2021, 11, 14218-14228.	3.6	14
8	Heterogeneity induced dual luminescence properties of AgInS ₂ and AgInS ₂ –ZnS alloyed nanocrystals. Inorganic Chemistry Frontiers, 2021, 8, 3450-3462.	6.0	8
9	Caffeine-Cyclodextrin Complexes as Solids: Synthesis, Biological and Physicochemical Characterization. International Journal of Molecular Sciences, 2021, 22, 4191.	4.1	6
10	Boosting the Catalytic Performance of Co/Mg/La Catalyst for Ammonia Synthesis by Selecting a Pre-Treatment Method. Catalysts, 2021, 11, 941.	3.5	13
11	1D and 2D hybrid polymers based on zinc phenylphosphates: synthesis, characterization and applications in electroactive materials. RSC Advances, 2021, 11, 7873-7885.	3.6	3
12	On the Sensitivity of the Ni-rich Layered Cathode Materials for Li-ion Batteries to the Different Calcination Conditions. Nanomaterials, 2020, 10, 2018.	4.1	33
13	Kinetic studies of ammonia synthesis over a barium-promoted cobalt catalyst supported on magnesium–lanthanum mixed oxide. Journal of the Taiwan Institute of Chemical Engineers, 2020, 114, 241-248.	5.3	16
14	Addition of yttrium oxide as an effective way to enhance the cycling stability of LiCoO2 cathode material for Li-ion batteries. Solid State Ionics, 2020, 355, 115426.	2.7	19
15	From Ag ₂ S to luminescent Ag–In–S nanocrystals <i>via</i> an ultrasonic method – an <i>in situ</i> synthesis study in an NMR tube. Journal of Materials Chemistry C, 2020, 8, 8942-8952.	5.5	8
16	Different strategies of introduction of lithium ions into nickel‑manganese‑cobalt carbonate resulting in LiNi0.6Mn0.2Co0.2O2 (NMC622) cathode material for Li-ion batteries. Solid State Ionics, 2020, 348, 115273.	2.7	22
17	Investigation of different ways of activation of fly ash–cement mixtures. Journal of Thermal Analysis and Calorimetry, 2019, 138, 4203-4213.	3.6	23
18	Synthesis of CuFeS2â^'xSex – alloyed nanocrystals with localized surface plasmon resonance in the visible spectral range. Journal of Materials Chemistry C, 2019, 7, 6246-6250.	5.5	14

ANDRZEJ OSTROWSKI

#	Article	IF	CITATIONS
19	Highly Luminescent Ag–In–Zn–S Quaternary Nanocrystals: Growth Mechanism and Surface Chemistry Elucidation. Inorganic Chemistry, 2019, 58, 1358-1370.	4.0	27
20	Thermally induced structural transformations of linear coordination polymers based on aluminum tris(diorganophosphates). Dalton Transactions, 2018, 47, 16480-16491.	3.3	5
21	Facile Gram-Scale Synthesis of the First n-Type CuFeS2 Nanocrystals for Thermoelectric Applications. European Journal of Inorganic Chemistry, 2017, 2017, 3150-3153.	2.0	17
22	Luminophores of tunable colors from ternary Ag–In–S and quaternary Ag–In–Zn–S nanocrystals covering the visible to near-infrared spectral range. Physical Chemistry Chemical Physics, 2017, 19, 1217-1228.	2.8	29
23	Linear coordination polymers based on aluminum phosphates: synthesis, crystal structure and morphology. Dalton Transactions, 2016, 45, 8008-8020.	3.3	6
24	Microwave Plasma Chemical Vapor Deposition of SbxOy/C negative electrodes and their compatibility with lithium and sodium Hückel salts—based, tailored electrolytes. Electrochimica Acta, 2016, 210, 395-400.	5.2	18
25	Non-injection synthesis of monodisperse Cu–Fe–S nanocrystals and their size dependent properties. Physical Chemistry Chemical Physics, 2016, 18, 15091-15101.	2.8	23
26	Understanding of Lithium 4,5-Dicyanoimidazolate–Poly(ethylene oxide) System: Influence of the Architecture of the Solid Phase on the Conductivity. Journal of Physical Chemistry C, 2016, 120, 23358-23367.	3.1	8
27	Cu–Fe–S Nanocrystals Exhibiting Tunable Localized Surface Plasmon Resonance in the Visible to NIR Spectral Ranges. Inorganic Chemistry, 2016, 55, 6660-6669.	4.0	39
28	Synthesis and crystal growth of microcrystals of the cubic and new orthorhombic polymorphs of (NH4)2SnCl6. Crystal Research and Technology, 2015, 50, 764-768.	1.3	4
29	Solvent effect in the synthesis of Cu–In–S and Cu–In–Se nanocrystals with tunable structure and composition. Materials Chemistry and Physics, 2015, 162, 291-298.	4.0	5
30	Synthesis and surface chemistry of high quality wurtzite and kesterite Cu2ZnSnS4 nanocrystals using tin(ii) 2-ethylhexanoate as a new tin source. Chemical Communications, 2015, 51, 12985-12988.	4.1	24
31	Ligand exchange in quaternary alloyed nanocrystals – a spectroscopic study. Physical Chemistry Chemical Physics, 2014, 16, 23082-23088.	2.8	38
32	A Simple Route to Alloyed Quaternary Nanocrystals Ag–In–Zn–S with Shape and Size Control. Inorganic Chemistry, 2014, 53, 5002-5012.	4.0	52
33	Effect of indium precursor and ligand type on the structure, morphology and surface functionalization of InP nanocrystals prepared by gas–liquid approach. Synthetic Metals, 2014, 187, 94-101.	3.9	4
34	Solid-state structure of methyl 2,4,6-tri-O-acetyl-3-O-(2,3,4,6-tetra-O-acetyl-β-d-glucopyranosyl)-β-d-galactopyranoside and methyl 3,4,6-tri-O-acetyl-2-O-(2,3,4,6-tetra-O-acetyl-β-d-glucopyranosyl)-β-d-galactopyranoside. Journal of Molecular Structure, 2013, 1037, 49-56.	3.6	3
35	Single-crystal and powder X-ray diffraction, 13C CP/MAS NMR, and DFT-GIAO calculations of methyl 3,4,6-tri-O-acetyl-2-O-(2,3,4,6-tetra-O-acetyl-12-d-galactopyranosyl)-1±-d-glucopyranoside and methyl 2,4,6-tri-O-acetyl-3-O-(2,3,4,6-tetra-O-acetyl-12-d-galactopyranosyl)-1±-d-glucopyranoside. Journal of Molecular Structure. 2013. 1036. 407-413.	3.6	2
36	Crystal and molecular structure of nitrophenyl 2,3,4-tri-O-acetyl-Î ² -d-xylopyranosides. Journal of Molecular Structure, 2012, 1007, 227-234.	3.6	1

#	Article	IF	CITATIONS
37	Solid-state structure of N-o-, N-m-, and N-p-nitrophenyl-2,3,4-tri-O-acetyl-β-d-xylopyranosylamines. Carbohydrate Research, 2011, 346, 2491-2498.	2.3	2
38	Effects of compositional and structural features on corrosion behavior of nickel–tungsten alloys. Journal of Solid State Electrochemistry, 2009, 13, 263-275.	2.5	63
39	Single-crystal and powder X-ray diffraction and solid-state 13C NMR of p-nitrophenyl glycopyranosides, the derivatives of d-galactose, d-glucose, and d-mannose. Carbohydrate Research, 2009, 344, 1734-1744.	2.3	11
40	Organically Modified Aluminophosphates:  Transformation of Boehmite into Nanoparticles and Fibers Containing Aluminodiethylphosphate Tectons. Chemistry of Materials, 2007, 19, 5584-5592.	6.7	18
41	GaN growth by sublimation sandwich method. Physica Status Solidi C: Current Topics in Solid State Physics, 2005, 2, 1065-1068.	0.8	0